

The development of
thermal hydraulic models to address specific problems
in pressurized water reactors

by

James D. Kegy

A Thesis Submitted to the
Graduate Faculty in Partial Fulfillment of the
Requirements for the Degree of
MASTER OF SCIENCE

Major: Nuclear Engineering

Signatures have been redacted for privacy

Iowa State University
Ames, Iowa

1982

TABLE OF CONTENTS

	Page
I. INTRODUCTION	1
A. Preamble	1
B. Statement of the Problem and Its Importance	2
II. LITERATURE REVIEW	4
III. PRELIMINARY CONSIDERATIONS TO MODEL DEVELOPMENT AND VERIFICATION	6
A. Introduction	6
B. Computer Code COBRA-IV-1	7
C. Data	9
IV. SMALL MODEL	10
A. Development	10
1. Channels	10
2. Rods	12
3. DNBR correlation	15
B. Verification	19
1. Lateral momentum factor	20
2. Friction coefficient K_{1j}	21
3. Internal to external iterations	22
4. Axial nodes	25
C. Conclusion	26
V. LARGE T-H MODEL	27
A. Introduction	27
B. COBRA-IV-1 Modeling	28
1. Channels	28
2. Rods	29

	<u>Page</u>
3. Thermal hydraulic parameters	31
a. Inlet flow distribution	32
b. Critical heat flux correlation	32
c. Pressure loss coefficient	32
C. Computer Selection	32
D. Analysis	33
1. Hot zero power	33
2. Nominal conditions; power adjusted to MDNBR	35
3. Flow reduction	35
4. Fluid density reduction	35
E. Conclusion	39
VI. CONCLUSIONS AND SUGGESTIONS FOR FUTURE WORK	40
A. Conclusions	40
B. Suggestions for Future Work	40
VII. LITERATURE CITED	42
VIII. ACKNOWLEDGMENTS	45
IX. APPENDIX A: EXXON NUCLEAR COMPANY FUEL DATA	46
X. APPENDIX B: COMBUSTION ENGINEERING FUEL DATA	60

LIST OF FIGURES

		<u>Page</u>
Figure 4.1	Small thermal hydraulics model	11
Figure 4.2	Internal iterations versus CPU time	24
Figure 5.1	COBRA-IV-1 double octant model	30
Figure 9.1	ENC fuel assembly geometry	48
Figure 9.2	ENC hot assembly flow areas	49
Figure 9.3	ENC matrix subchannel	50
Figure 9.4	ENC side subchannel	51
Figure 9.5	ENC corner subchannel	52
Figure 9.6	Subchannel between two ENC assemblies	53
Figure 9.7	Subchannel between one ENC assembly and one CE assembly	54
Figure 9.8	Subchannel surrounded by four ENC assemblies	55
Figure 9.9	ENC gap connections	56
Figure 9.10	ENC matrix subchannel gap connections	57
Figure 9.11	ENC gap connections for side and corner subchannels	58
Figure 9.12	Relative spacer grid locations	59
Figure 10.1	CE fuel assembly geometry	62
Figure 10.2	CE hot assembly flow areas	63
Figure 10.3	CE matrix subchannel	64
Figure 10.4	CE side subchannel	65
Figure 10.5	CE corner subchannel	66
Figure 10.6	Subchannel surrounded by four CE assemblies	67

LIST OF TABLES

		Page
Table 4.1	COBRA-IV-I small model subchannel input data	13
Table 4.2	COBRA-IV-I small model rod input data	16
Table 4.3	Small model s/l sensitivity	21
Table 4.4	Small model K_{ij} sensitivity	22
Table 4.5	Small model iteration optimization	23
Table 4.6	Small model axial node optimization	25
Table 5.1	Hot zero power comparison	34
Table 5.2	Nominal pressure - Temperature - Flow Overpower to MDNBR	36
Table 5.3	Flow reduction comparison	37
Table 5.4	Density reduction comparison	38
Table 9.1	Key neutronic design parameters for Fort Calhoun XN-1 type H fuel	47
Table 10.1	Key neutronic design parameters for Fort Calhoun CE type G fuel	61

I. INTRODUCTION

A. Preamble

Thermal-hydraulic (T-H) computer codes are used to predict the way coolant flows through a reactor core. This is especially important since the coolant transfers the heat from the fuel pins to the steam generators. These codes must predict this behavior for a wide variety of plant operating conditions and also provide information on both rapid and very slow developing transients.

For all of these situations, it is important to know how the heat is being removed from the fuel pins. Therefore, T-H codes must account for crossflows from one subchannel to another and for fluid interaction among fuel assemblies. Additionally, a number of other conditions must be taken into account. Some of these include inlet flow distributions at the bottom of the core and exit pressure distributions and the top of the core. In general, anything that could affect the flow pattern in the core or impact the heat transfer process must be included in the model.

The single most important function that a hydraulics code can perform is the prediction of those conditions where fuel pins could experience departure from nucleate boiling (DNB). The fuel pins consist of a ceramic fuel material and an outside cladding material, usually a zirconium alloy. When the coolant goes through DNB, the temperature rises causing the clad to lose its structural integrity,

allowing fission gases and fuel material to "escape" into the coolant. To prevent the fuel from reaching DNB, a nuclear power plant is operated with a set of Limiting Conditions of Operation (LCOs). The LCOs arise from a set of assumption leading to bounding conditions that must be maintained to insure the validity of the setpoints. The T-H codes play a vital role in the development of the LCOs and the setpoints that are used in the RPS.

Analyses, performed using the thermal hydraulic codes, must be run many times to examine the response of the core to a range of plant operating conditions. The model detail can range from modeling every pin and subchannel in the core, to modeling only one pin and one subchannel. The larger the model, the greater the cost of using it. The smaller the model, the more limited the information. Given the cost of large models, it has become crucial to develop models that are small enough to be inexpensive to run and at the same time still provide adequate information about the behavior of the core.

B. Statement of the Problem and Its Importance

The source of the data for this research project was the Ft. Calhoun Station Unit No. 1 reactor which is operated by the Omaha Public Power District. The Ft. Calhoun unit is a 500MW electric pressurized water reactor located near Blair, Nebraska.

The purposes of the study were to:

- (1) Develop a small hydraulic model that explicitly models one-sixteenth of the "hottest" assembly in the core and doesn't model the balance of the core.
- (2) use the small model to verify the thermal margin/low pressure settings already in use at the unit for the current core loading (Cycle 6).
- (3) develop a larger model that explicitly models all of the interconnecting channels of two adjacent assemblies and one-eighth of each of the assemblies.
- (4) investigate, using the larger model, the effect that placing two assemblies with different grid types in adjacent locations would have on crossflows between them.

The development of hydraulics models designed for specific purposes, can be of considerable value to a utility. The models can be developed at a minimum of cost and the analysis can be conducted by an "in house" staff. This provides the utility with the ability to perform the work within their own time frame and to forego the additional expense of contracting the work to a private vendor.

II. LITERATURE REVIEW

A variety of thermal hydraulic (T-H) computer codes are available for utilities that own and operate pressurized water reactors (PWRs) (1). Several are a direct growth of the work at Northwest Battelle Laboratories (2) on the COBRA series (2-7). T-H codes can be grouped as public access codes (2-5) and as proprietary codes (6-9).

The rights on proprietary codes are usually held and developed by private nuclear service companies such as Combustion Engineering and Exxon Nuclear Corporation. These companies can provide the user with an array of technical support services to complement the codes. Public access codes are generally available to the user at less cost but the user may need more "in house" expertise to maximize a particular code's potential. Public access codes also have the advantage of the availability of the source deck; allowing for modification of the code.

One code, COBRA-IV-1 (2-3), has a dimensioning routine that permits redimensioning the entire code to the exact size of the hydraulics model. This provides both a computer savings, by not allocating unnecessary storage space, and permits extremely large models to be handled by the code.

T-H codes are used to predict both steady state and transient behavior in the reactor core. For these predictions, the selection of the proper critical heat flux (CHF) correlation (10-12) is

important. These correlations predict the approach of the fuel to the minimum departure from nucleate boiling ratio (MDNBR). The widest use of T-H codes is in the generation of setpoints (13-15) to ensure that the MDNBR ratio is never exceeded.

T-H codes can also be used to investigate core hydraulic responses to special problems that might arise on short notice. Often a utility hires a private nuclear service company to generate the setpoints for a reactor protective system. If a utility wanted to verify those setpoints (16), an inexpensive, simple T-H would be beneficial.

III. PRELIMINARY CONSIDERATIONS TO MODEL DEVELOPMENT AND VERIFICATION

A. Introduction

When the operators of a nuclear power plant need thermal-hydraulic information on the reactor core, it can be required under a variety of circumstances. In the case of verifying the conservatism of reactor protective setpoints, it can be an on-the-spot verification of degradation of the system or a time consuming verification of the reload analysis. In either case, a quick running conservative calculation of departure from nucleate boiling (DNB) is required. This type of model needs to be inexpensive to execute, since setpoint verification, like setpoint generation, requires a large number of cases (up to several thousand).

Another type of thermal-hydraulic model that can be required is the very extensive, expensive-to-run model designed to perform one particular task. Since this type of model will stress the large core memory (LCM) limits of a computer system to the maximum, it is well worth the time to develop a model and optimize it wherever possible and set it up on a computer that is large enough to handle all code details. The LCM capacity of a computer is stressed because most T-H codes require capacity based on a model limit and the needs of all the options available in the code, whether or not they are called upon.

The purpose of this work was to develop two thermal-hydraulic models with vastly different sizes and purposes. Because of the differences in purpose, the ability of models to function properly was tested on an individual basis. Due to the completely unique nature of the larger of the two models, some time is devoted to an explanation of its use.

The first model was a small model (only the barest of essentials were included). This model had a short execution time (partly through enhancements). This model had to be capable of being run many times with a minimum of change and at the least cost.

The second model was an especially large model. It consisted of the exact modeling of one-eighth of each of two adjacent fuel assemblies and the region between them. This model required extensive LCM and computer time for each case.

B. Computer Code COBRA-IV-1

The first step in the design of the T-H models was the selection of the computer code to be used in conjunction with the models. The COBRA-IV-1 (3,4) code was selected for the following reasons:

1. The computer code is a public access code developed at a national laboratory (BNL) (3,4). As such, it is available to all types of users at minimum cost. In general, the only real expenses are related to the running of the cases.

2. Because the code is in the public domain, the source deck for the code is accessible. This permits the user to modify, add or delete subroutines at his discretion. The proprietary codes must be used in an "as is" condition unless special arrangements are made with the code owner.

3. The COBRA-IV-1 code has versions that can be loaded in many large computers including IBM, CDC, UNIVAC, and the CRAY 1.

4. One of the real bonuses of COBRA is the SPECSET (4) subroutine. SPECSET provides the user with the ability to redimension the entire code to the exact size of the model being incorporated into the code. This minimizes the computer core storage requirements. This enables the code to efficiently handle both very large and very small models.

5. If the requirements of the case exceed the LCM capabilities of a computer system, the code has a peripheral storage option permitting partial results to be stored on tape, and the LCM cleared. The problem can then be continued from the tape file of partial results. This is a time consuming and costly option, but it may allow larger models to be run on a computer of limited LCM.

6. If the user needs to do a parametric study, this code also has a restart function. This option permits the code to be initialized (restarted) from the results from the previous case; thus, reducing the number of calculations for subsequent runs.

C. Data

The data used in the construction of the models were based on Ft. Calhoun Nuclear Station Unit No. 1, owned and operated by the Omaha Public Power District located at Omaha, Nebraska (17). The unit is rated at 1500MWth. The initial fuel supplier was Combustion Engineering (CE). The present supplier of reload fuel is the Exxon Nuclear Company (ENC). The basic data for the ENC fuel are provided in Appendix A "ENC Fuel Data" and the CE fuel data are in Appendix B "CE Fuel Data".

IV. SMALL MODEL

A. Development

The small model was designed to use the least computer core memory and to be executed very rapidly. It was intended for use as a verification of fuel reload setpoints and as such was a DNBR calculator. An example of a small model is the COBRA-III-C (2) model used by Yankee Atomic Electric Company (13) which models the "hottest" subchannel and its nearest neighbors explicitly. The balance of the assembly is then combined as one rod and one subchannel. The remaining one-eighth of the core is modeled as the last rod and subchannel. Other examples are the CE S-TORC (18) and CETOP small models (9) which also use combination of assemblies into single subchannels and fuel rods.

1. Channels

The model presented in this work does not, however, use any combining of larger groups of subchannels and fuel rods; nor does it describe them explicitly. Since the model was only for DNBR calculations and previous setpoint verification, it was only designed to model the "hottest" subchannel in the core and its nearest neighbors. For conservative calculations, this is not an unreasonable assumption. An MIT-EPRI study (5) shows that the representation of the first neighbors has a significant effect on results, but second and third neighbors do not alter the results. Figure 4.1 illustrates the model.

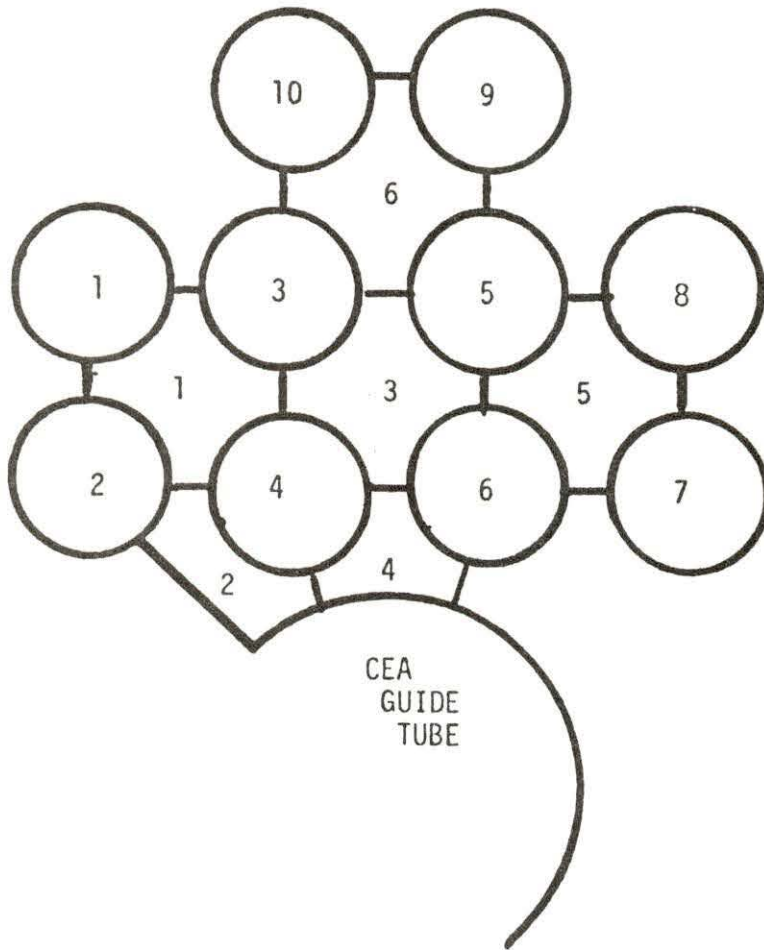


Figure 4.1 Small thermal hydraulics model

The numbered boxes represent the subchannels and the numbered circles the fuel rods. For calculational purposes, channel 3 and rod 4 were considered to be the "hot" candidates. The code input information was taken from Appendix A, "ENC Fuel Data".

Subchannels 1, 3, 5, and 6 were matrix subchannels. Subchannel 3 was one-half of a corner subchannel and subchannel 4 is a side subchannel. The basic subchannel input data are given in Table 4.1.

2. Rods

The six subchannels were surrounded by ten fuel rods and part of a guide tube. An ENC fuel rod has a diameter of 0.442 inches and the guide tube has a diameter of 1.115 inches. The radial power distribution was based on a typical beginning of cycle "hot" assembly power distribution, scaled to the Technical Specification limit (19) for full power operation.

The other input parameter associated with the fuel rods, was the fraction of energy deposited in the flow channels adjacent to the fuel rods. This is typically the geometric fraction (f_{ij}) of the rod facing the subchannel. Since the model was developed for direct calculational verification, certain other adjustment factors were applied to the f_{ij} 's,

Some of the factors used were:

1. Engineering enthalpy rise factor ($F_{\Delta H}$). This factor was applied to the rods that surround the "hot" subchannel. This increased

Table 4.1 COBRA-IV-I small model subchannel input data

Channel No.	Flow Area (in ²)	Wetted Perimeter inches	Heated Perimeter inches	Channel to Channel Connect.		
1	.1830	1.389	1.389	.1380(2)	.1380(3)	
2	.1149	.8575	.5920	.1385(4)		
3	.1830	1.389	1.389	.1380(4)	.1380(4)	.1380(6)
4	.0913	.9108	.5521			
5	.1830	1.389	1.389			
6	.1830	1.389	1.389			

the enthalpy rise for the entire length of the "hot" subchannel without changing the local heat flux at the surface of the rod.

2. Engineering heat flux factor (F_Q). This factor accounted for increases in the local heat flux due to manufacturing and fabrication tolerances of the pellets and clad. This factor was applied to the "hot" rod.

3. The third factor included was to account for the fraction of thermal power produced in the fuel (F_γ). This factor was applied to all of the rods in the model.

Typical values used for these factors are (17):

$$F_{\Delta H} = 1.03$$

$$F_Q = 1.03$$

$$F_\gamma = .975.$$

The calculations for each rod follow (13). The first subscript indicates the rod number and the second the subchannel.

The "hot" rod fraction to the "hot" subchannel (3) is

$$F_{ij} = f_{ij} F_{\Delta H} / F_Q F_\gamma \quad [1]$$

$$F_{43} = .25(1.03/(1.03)(.975)) = .2564.$$

The other "hot" rod fractions are:

$$F_{ij} = f_{ij} / (F_{\gamma})(F_Q) \quad [2]$$

$$F_{41} = .25 / (1.03)(.975) = .2489$$

$$F_{42} = .3012 / (1.02)(.973) = .2999$$

$$F_{44} = .1988 / (1.03)(.975) = .1980$$

The fractions for the other rods depositing energy into the "hot" subchannel were:

$$F_{ij} = f_{ij} F_{\Delta H} / F_{\gamma} \quad [3]$$

$$F_{33} = .25(1.03) / .975 = .2641$$

$$F_{53} = .25(1.03) / .975 = .2641$$

$$F_{63} = .25(1.03) / .975 = .2641.$$

The remaining rod fractions were calculated by the following formula:

$$F_{ij} = f_{ij} / F_{\gamma} \quad [4]$$

The rod input data are summarized in Table 4.2.

3. DNBR correlation

The DNBR correlation used with the small T-H model and the COBRA-IV-1 code was the W-3 (1.3 MDNBR) correlation (1) including

Table 4.2 COBRA-IV-I small model rod input data

Rod #	Rod Diameter Inches	Radial Power Factor	Fraction of Power to Adjacent Channels (Adjacent Channel)			
1	.442	1.440	.2564(1)			
2	.442	1.520	.2564(1) .1558(2)			
3	.442	1.485	.2564(1) .2641(3) .2564(6)			
4	.442	1.66	.2489(1) .2999(2) .2564(3) .1980(4)			
5	.442	1.479	.2641(3) .2564(5) .2564(6)			
6	.442	1.562	.2641(3) .2031(4) .2564(5)			
7	.442	1.517	.2564(5)			
8	.442	1.464	.2564(5)			
9	.441	1.389	.2564(6)			
10	.442	1.386	.2564(6)			

corrections for nonuniform axial heat flux (F_s) and the unheated boundary (cold wall effect) given as Equation 5.

For uniformly heated channels, the critical heat flux $q''_{crit,EU}$, is given by:

$$\frac{q''_{crit,EU}}{10^6} = \{(2.022 - 0.0004302P) + (0.1722 - 0.0000984P) [5]$$

$$X \exp[(18.177 - 0.004129P)\chi]\}$$

$$X [(0.1484 - 1.596\chi + 0.1729\chi|\chi|)G/10^6 + 1.037]$$

$$X [1.157 - 0.869\chi]X[0.2664 + 0.8357 \exp(-3.151D_e)]$$

$$X [0.8258 + 0.000794 (H_{sat} - H_{in})]F_s,$$

where

F_s = grid or spacer factor

P = 1000 to 2300, psia

G = 1.0×10^6 to 5.0×10^6 , lb/(h ft²)

D_e = 0.2 to 0.7, in.

$\chi_{loc} \leq 0.15$

$H_{in} \geq 400$ Btu/lb

L = 10 to 144 in.

Equation 5 is restricted to the range

$$\frac{\text{heated perimeter}}{\text{wetted perimeter}} = 0.88 \text{ to } 1.00.$$

The correlation has a correction for nonuniform axial heat flux given by:

$$q''_{\text{crit},N} = q''_{\text{crit},EU}/F \quad [6]$$

where

$q''_{\text{crit},N}$ = DNB heat flux for the uniformly heated channel

$q''_{\text{crit},EU}$ = equivalent uniform DNB flux from Eq. (5)

$$F = \frac{C}{q''_{\text{local}}} \int_0^{\ell_{\text{DNB},N}} q''(z) \exp[-C(\ell_{\text{DNB},N} - z)] dz$$

$$C = 0.44 \frac{(1 - \chi_{\text{DNB}})^{7.9}}{(G/10^6)^{1.72}} \text{ in.}^{-1} \quad [7]$$

$\ell_{\text{DNB},EU}$ = axial location at which DNB occurs for uniform heat flux, in.

$\ell_{\text{DNB},N}$ = axial location at which DNB occurs for nonuniform heat flux, in.

χ_{DNB} = quality at DNB location under nonuniform heat flux conditions.

The cold wall effect arises from the nonuniform enthalpy across a subchannel that is not being heated from all sides. The correction for this effect is given by:

$$q''_{\text{crit},EU,CW} = (q''_{\text{crit},EU,D_h})_{\text{CWF}},$$

where

q''_{crit,EU,D_h} = critical heat flux evaluated from Eq. (5)

with D_h replacing D_e

$$\begin{aligned}
 D_h &= \text{equivalent diameter based on heated perimeter, in.} \\
 q''_{\text{crit,EU,CW}} &= \text{critical heat flux in presence of cold wall} \\
 \text{CWF} &= 1 - \text{Ra} [13.76 - 1.372 \exp(1.78X) - 4,732 (G/10^6)^{-0.0535} \\
 &\quad - 0.0619 (P/10^3)^{0.14} - 8,509 D_h^{0.107}] \quad [8] \\
 \text{Ra} &= 1 - (D_e/D_h).
 \end{aligned}$$

The correlation was devised for:

$$\begin{aligned}
 x_{\text{DNB}} &\leq 0.1 \\
 1.0 \times 10^6 &\leq G \leq 5.0 \times 10^6 \\
 1000 \text{ psia} &\leq P \leq 2300 \text{ psia} \\
 L = \text{heated length} &\geq 10 \text{ in.} \\
 \text{gap} &\geq 0.1 \text{ in.}
 \end{aligned}$$

When the axial heat flux is nonuniform, the predicted critical heat flux is given by:

$$q''_{\text{crit,N,CW}} = \frac{(q''_{\text{crit,EU,D}_h}) \text{CWF}}{F} \quad [9]$$

B. Verification

The model verification consisted of two parts. The first part concerned the sensitivity of the results to several input parameters (lateral momentum factor, lateral friction coefficient). These are important since they are not calculated in the code for each sub-channel pair, and only one value for each can be used. It is

imperative that the DNB calculations not be affected by the range of values used for these parameters.

The second area for verification was to determine the most economical manner to run the code and still get conservative values for DNBR. This involved a comparison of combinations of internal to external iterations, and the optimum number of axial nodes.

1. Lateral momentum factor

The basic transverse momentum equation in COBRA-IV-1 has not been altered from COBRA-III-C (4). For simplification, consider only two interconnection subchannels of relatively equal area (a good assumption for this model). The lateral momentum matrix is then given by (2):

$$m = 1/\Delta t + u^*/\Delta x + s/\ell (C) + (s/\ell)[2u^*/A](\Delta x) \quad [10]$$

where:

A = cross sectional area of the unit cell

Δx = thickness of the unit cell

u^* = average velocity of the two subchannels

C = transverse friction term

D. S. Rowe (2) discusses the impact of the parameter (s/ℓ) on the lateral momentum calculation and notes that it is normally not a sensitive parameter. The s value represents the gap connection between two adjacent subchannels, and is equal to the centroid

distance associated with the two subchannels. For a pair of matrix subchannels, this ratio would be $.138/.58 = .2379$. To verify that the model was insensitive to the parameter in question, several cases were run over a range of s/ℓ from .2 to 2.0. The results are shown in Table 4.3.

Table 4.3. Small model s/ℓ sensitivity

s/ℓ :	Hot Channel Enthalpy Rise BTU/lb _M	W-3 MDNBR	Hot Rod
.02	145.28	1.289	4
.4	145.32	1.289	4
2.0	145.34	1.289	4

The MDNBR and the hot channel enthalpy rise both proved to be insensitive to wide variations in s/ℓ .

2. Friction coefficient K_{ij}

From the transverse momentum equation (Eq. 10), the smallest term is usually C, the transverse friction term (2). If the spacing of the rods was extremely close, then K_{ij} could increase considerably since it is approximately proportional to one over the spacing. Note, K_{ij} is modeled in the C term. Although this term should be small for gap spacings on the order of .1380 -

.1385 inches, an analysis was conducted that it did not present a problem. As can be seen from the results in Table 4.4, even over a wide range, none of the outputs of interest changed.

Table 4.4 Small model K_{ij} sensitivity

K_{ij}	Hot Channel Enthalpy Rise BTU/lb _M	Hot Channel Pressure Drop PSI	MDNBR	Hot Rod
.01	145.32	14.92	1.289	4
.1	145.32	14.92	1.289	4
1	145.32	14.92	1.289	4

3. Internal to external iterations

Since the convergence criteria were not changed for either of the iteration types, the same MDNBR is always attained. The only question was, "What is the least costly combination of internal and external iterations?" i.e. does it cost more to iterate more times at each plane or is it more expensive to go from the bottom of the model to the top more times? Table 4.5 summarizes the various combinations tried. The asterisk (*) indicates that the external convergence criteria were not satisfied although the number limit was reached. Although forty external iterations were never used, the code was given this window to ensure meeting the tolerance criteria. Figure 4.2 shows the cost for 40 external iterations in

Table 4.5 Small model iteration optimization

<u>LIMITS</u>	<u>ITERATIONS</u>	<u>ACTUAL</u>	MDNBR	CPU time
External	Internal	External	For each Case	(sec)
20	20	*	1.364	2.787
30	10	*	1.364	3.494
30	29	25	1.364	3,297
30	30	29	1.364	2.932
40	29	25	1.364	2.297
40	30	20	1.364	2.993
40	40	17	1.364	2.695
40	50	15	1.364	2.493
40	60	13	1.364	2.256
40	90	10	1.364	1.805
40	100	9	1.364	1.743
40	120	9	1.364	1,826
40	150	8	1.364	1.740
40	170	8	1.364	1.742
40	220	8	1.364	1.743
5	150	*	1.364	1.330
10	150	8	1.364	1.740
15	150	8	1.364	1.739
20	150	8	1.364	1.740
25	150	8	1.364	1.739

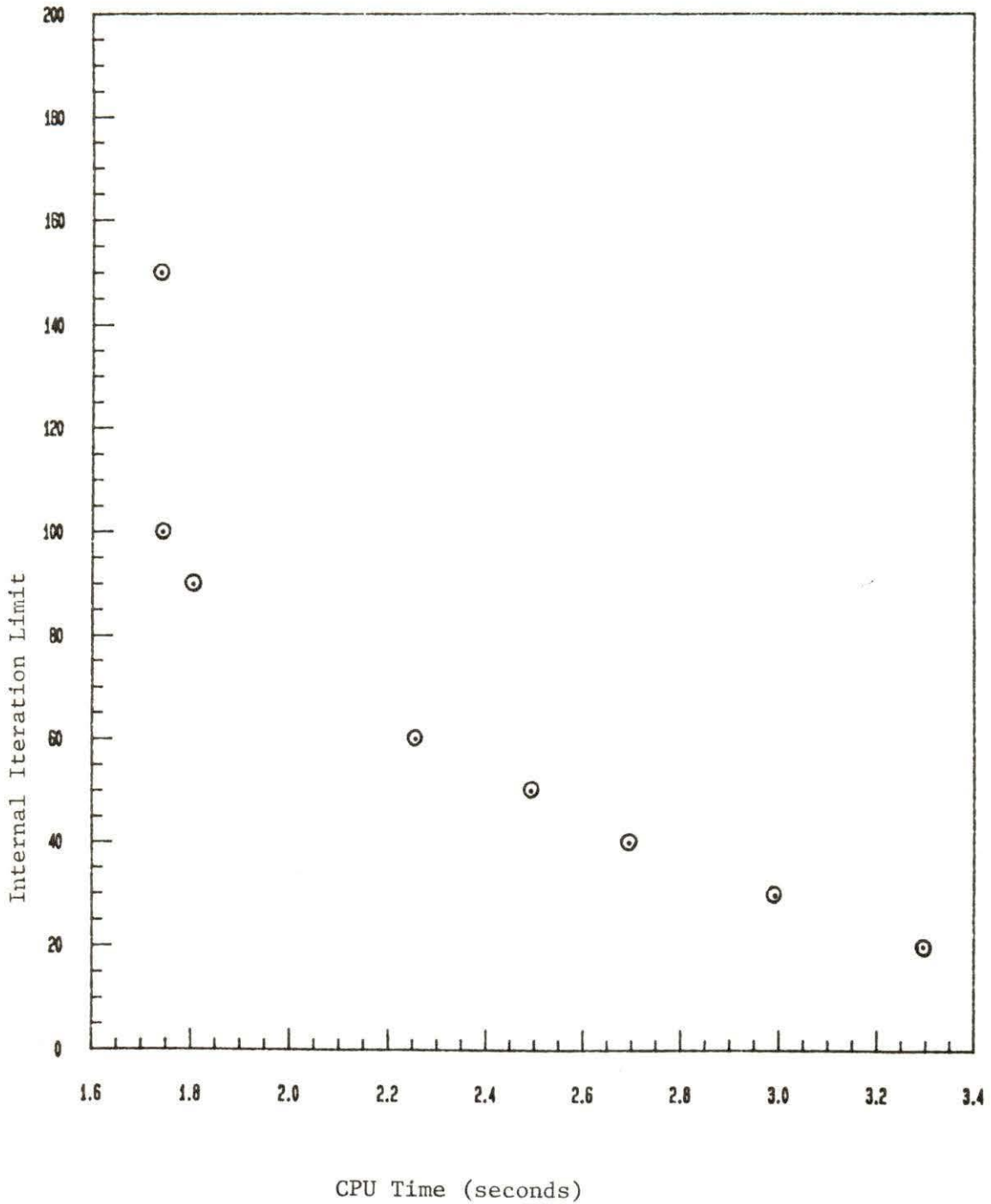


Figure 4.2 Internal iterations versus CPU time

conjunction with a variety of internal limits. A combination of 40 external iterations together with 150 internal iterations was almost twice as cheap as the 40 external iterations with 20 internal iterations. This was due to the actual number of external iterations required for each case.

4. Axial nodes

The trade-off on the number of axial nodes versus the cost of each computer run was found by finding the most economic combination. Table 4.6 summarizes the results.

Table 4.6 Small model axial node optimization

# of Axial Nodes	Node Length Inches	cpu sec.	MDNBR	"Hot" rod
10	12.8	3.404	1.569	4
20	6.4	2.703	1.524	4
30	4.2667	1.430	1.529	4
40	3.2	1.298	1.527	4
50	2.56	1.676	1.529	4

The first concern must always be the nodalization that yields the lowest MDNBR. Nodes sizes from 6.4" to 2.56" all predicted values within +.005 DNBR units of each other. This meant that they could

all be classified as equivalent since the DNB correlation was valid to a $\pm .005$ value (10). Of these four, the forty (4) node arrangement was the most efficient. It required the least (1.298 seconds) amount of computer time to determine the same result as the other axial models.

C. Conclusion

Two conclusions were drawn from this work on the development of a small T-H model for DNB verification and validation purposes.

The first conclusion is that a small thermal-hydraulic model can be developed for the purpose of DNBR verification. The most important observation is that this "simple" model could be used to conservatively model the "hot" channel and its nearest neighbors, while not considering anything else in the core.

The second conclusion is that a T-H model that would be used several thousand times for each analysis could be optimized for cost while not sacrificing any of its prediction capability. It was found that in the implicit solution scheme a "best" combination of internal and external limits existed. Additionally, the cost of a run was further dependent upon the axial node size. For the model, an internal limit of 150 iterations and an external limit of 40 iterations was determined to be the least expensive. Furthermore, based on the iteration scheme, the best node size was found to be 3.20 inches.

V. LARGE T-H MODEL

A. Introduction

For the initial five cycles, the Fort Calhoun Nuclear Power Station was fueled exclusively with Combustion Engineering (CE) fuel. For Cycle 6, forty Exxon Nuclear Company (ENC) fuel assemblies were loaded in the core. This "mixed" loading introduced an unknown into the analysis of the thermal hydraulic performance of the core. This unknown was the effect of having assemblies with different grid loss coefficients loaded into the core in adjacent locations.

Grid spacers contribute to the amount of pressure drop across each assembly in a reactor core. If fuel assemblies with different grid types were placed in adjacent locations in the core, the pressure drops would be different. This difference in pressure drop will contribute to the amount of crossflow between the two assemblies, since flow up the "hot" channel has considerable impact on the enthalpy rise of the "hot" channel (approach to critical heat flux). The amount of flow "starvation" that the "hot" channel experiences is of considerable importance in DNBR calculations. For example, if a "hot" ENC assembly (larger loss coefficient) was located next to a "colder" CE assembly (smaller loss coefficient) the net cross flow could be out of the ENC assembly and into the CE assembly. This would effectively reduce the flow into the "hot" assembly and cause a lower DNB for the same operating conditions.

B. COBRA-IV-1 Modeling

The purpose of this modeling is to isolate and examine the effect of grid spacer-types on crossflow. With this in mind, a double octant model was developed with each octant representing an assembly. Since only grid types are being examined, the model did not account for the two sizes of fuel rods (one type CE and one ENC) and the corresponding differences in hydraulic diameters, gaps, heated perimeters, wetted perimeters, flow areas, etc. The inputs used were the model based on values in Appendix B (CE fuel).

This model was developed only to examine the effect of two types of grids in adjacent assemblies and not to predict overall core performance.

The model was set up to approximate the minimum departure from nucleate boiling ratio (MDNBR) conditions. This was done because the effect of the grid on cross flow is of most interest when MDNBR conditions exist.

1. Channels

The COBRA-IV-1 model was set up as a double octant model with a total of sixty channels, as shown in Figure 5.1. Channels 1-26 constituted the first octant and channels 35-60 the second octant. The flow area between the octants is represented by channels 27-34. The large number of subchannel was chosen to give the grids (which holds the pins rigidly) an opportunity to drive the cross flow and then

observe if it has an effect on the "hot" subchannel or if the effect is cancelled as it moves through the assembly.

The "hot" channels in the first and second octant are twenty-four and thirty-nine, respectively.

2. Rods

The forty-eight (48) rod in the model (Figure 5.1) represents 48 individual rods. Pins 1 through 24 are mirrored by pins 25 through 48. This made the rod model for each octant identical. The peak-pin to 1/4 assembly relative power ratio was 1.11. A "flat" assembly is more limiting for MDNBR calculations. The peak rods are sixteen and thirty-six.

The complete input data for the rods in the model can be found in Appendix D.

The measured axial power distribution (ASI) represents the power in the upper half of the core (P_u) relative to the power in the bottom half of the core (P_L). This is calculated by:

$$ASI = \frac{P_L - P_u}{P_L + P_u}$$

Therefore, a negative ASI means that over half of the core power is generated in the top half of the core.

The negative normalized axial power distribution used was (ASI = -.182) with a maximum F_z value of 1.424. This distribution was uniformly applied to all 48 rods.

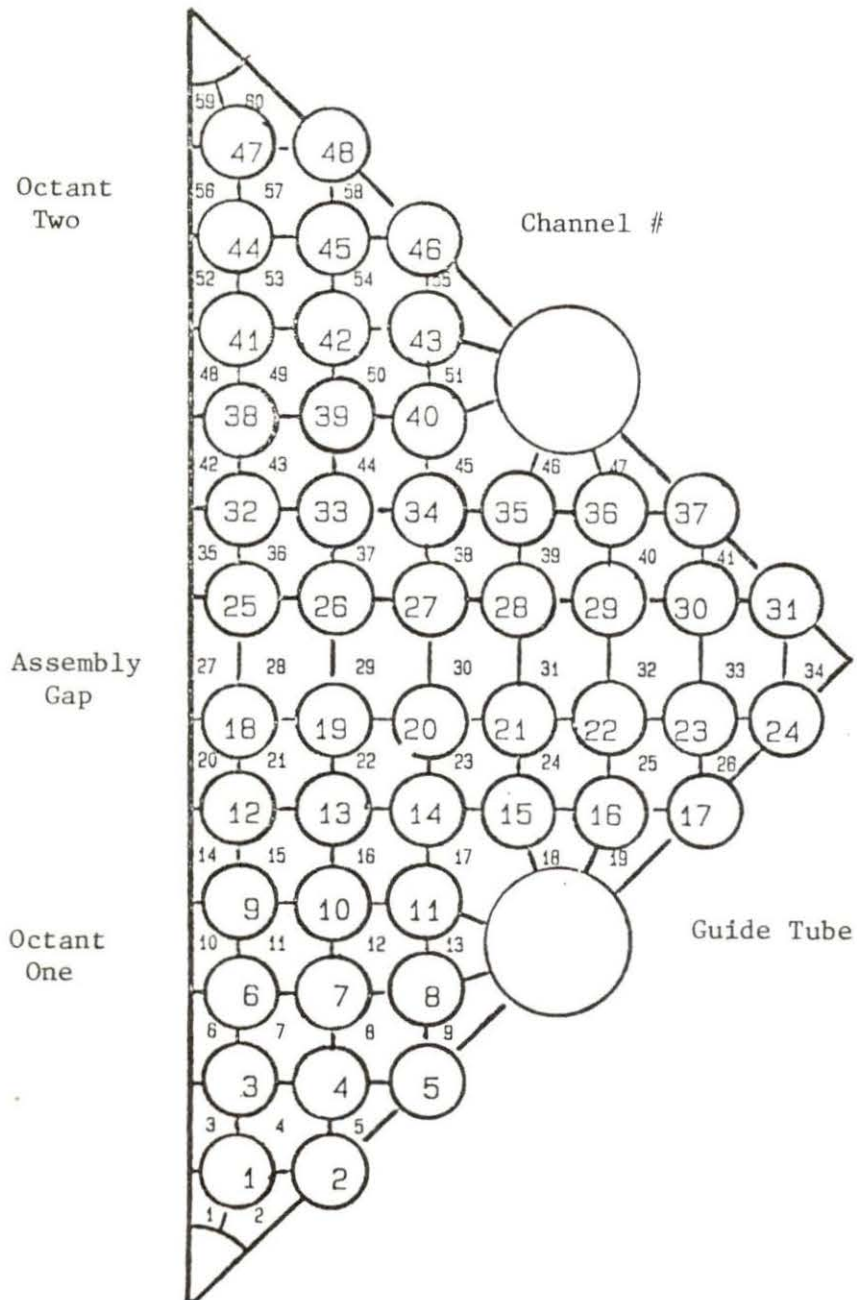


Figure 5.1 COBRA-IV-1 double octant model

The specific grid loss coefficients (ksg) used to represent ENC and CE assemblies were derived by Exxon Nuclear Company from actual flow measurements done with the test assemblies (20). The equations used for the two octants, each representing a different assembly, were:

$$\text{CE} - \text{Ksg} = 1.034 \text{ Re}^{-.04},$$

$$\text{ENC} - \text{Ksg} = 1.62 \text{ Re}^{-.067}.$$

For the grid loss coefficients, the code doesn't use calculated Reynolds numbers as inputs. Therefore, a conservative Reynolds number of 500,000 was chosen. The resulting inputs for CE and ENC octants were .61 and .67, respectively. The axial locations of the grids (Appendix A, B) are the same for both fuel types.

For the reference runs, both octants were always given the CE value of .62.

The geometric and "hot" channel factors were not applied in this study since only relative effects were of interest and the factors would be applied equally to both octants.

3. Thermal hydraulic parameters

Since conservatism was not an absolute criterion for this model, a number of the parameters discussed below could be called typical, although many would be unchanged if a conservative model had been the goal.

a. Inlet flow distribution The inlet flow for both octants was identical and uniform. The value used as nominal was the Fort Calhoun LCO value less bypass flow

$$195,700 \text{ GPM } (1-.0446) \frac{60 \text{ minutes}}{\text{Hour}} \frac{.13368 \text{ ft}^3}{\text{gal.}} \times \frac{47.05 \text{ lbm}^*}{\text{ft}^3}$$

$$32.68 \text{ ft.}^3$$

$$= 2.16 \times 10^6 \text{ lbm/Hr-ft}^2.$$

*Based on a pressure of 2075 psia and an inlet temperature of 545°F.

b. Critical heat flux correlation The 1.3 W-3 CHF correlation was used for calculating minimum DNBRs (21). For most of the cases examined, the minimum DNBR occurred in channel 39, although under some conditions it was predicted to occur in channel 46. This shift was due to the cold wall effect (22) that is included in the correlation.

c. Pressure loss coefficient The pressure losses due to rod friction was calculated as a function of Reynolds number. The friction factor correlation used was (21):

$$f = 0.199 R_e^{-0.2}$$

C. Computer Selection

After modeling was completed, a new problem had to be solved. The large model required over 900,000₈ words of LCM on a computer

The small model was run on a CDC-7600, but this machine only had 341,000₈ words of LCM. Use of the peripheral storage option was too expensive. Therefore, the large model was executed on a CRAY-I which had sufficient LCM. Also, the SPECSET subroutine had to be employed to dimension the code "up" to the increased size.

Due to the escalated cost of this type of analysis, cost optimization was not employed since it could have cost more than the analysis.

D. Analysis

For each case examined; the same procedure was followed. First, the run was made with both of the octants containing CE grids. The second run was made with the first octant containing CE grids and the second octant containing ENC grids. In each case, MDNBR was compared and the "hot" channel exit flow rates were compared. In all cases, the MDNBR occurred in the same "hot" channel.

1. Hot zero power

The first case examined the effect of the grids on cross flow with no heat addition in the core. This approximated a hot zero power condition since the system was pressurized and the inlet temperature was 545⁰F. The results (Table 5.1) showed that the "mixed" grid model had a 1.74% "hot" channel flow reduction. Since there was no heat addition DNBRs were not calculated.

Table 5.1 Hot zero power comparison

CASE	PRESSURE PSIA	TEMPERATURE °F	FLOW 10^6 lbm/ hr-ft ³	POWER % of Full Power	DENSITY lbm/ft ³	MDNBR 1.3 W-3 CHF Correlation	FLOW OUT OF "HOT" Channel lbm/hr-ft ²
BOTH OCTANTS CE	2075	545	2.1600	0.0	46.29	N/A	2.1503×10^6
ONE OCT CE ONE OCT ENC	2075	545	2.1600	0.00	46.29	N/A	2.1128×10^6

2. Nominal conditions; power adjusted to MDNBR

The second case was for nominal pressure, temperature, and flow values. For the all CE grid model, the power was raised until a 1.306 MDNBR was reached. The power level was 136% of full power (1500 MW(th)). These values were then used as the operating conditions for the mixed grid model. From Table 5.2, the MDNBR fell from 1,306 to 1.278 and the "hot" channel flow was reduced by 2.5%.

3. Flow reduction

One of the variables that affects heat transfer and, hence, MDNBR is the amount of flow in the channel. To observe the sensitivity of the mixed grid models flow reduction, a set of runs were made with the inlet flow reduced by 5%. The all CE grid model for a minimum MDNBR of 1.299 had a "hot" channel exit flow of 1.9654×10^6 lbm/ft²-hr. The conditions that yielded this result were input into the "mixed" grid model and the results given in Table 5.3 were obtained. The MDNBR dropped 2.2% and the "hot" channel exit flow was reduced by 2.3%.

4. Fluid density reduction

Another variable that has an impact on DNB is the density of the fluid. Less dense fluids reduce heat transfer, and as such represent more adverse conditions. To achieve the lower density, the inlet temperature was raised to 580^oF and the pressure was raised to 2400 psia. The results are given in Table 5.4. For the all CE grid model, the MDNBR was 1.307 and the "hot" channel exit flow was $2.0914 \times$

Table 5.2 Nominal pressure - Temperature - Flow
Overpower to MDNBR

CASE	PRESSURE PSIA	TEMPERATURE °F	FLOW 10^6 lbm/ hr-ft ³	POWER % of Full Power	DENSITY lbm/ft ³	MDNBR 1.3 W-3 CHF Correlation	FLOW OUT OF "HOT" Channel lbm/hr-ft ³
BOTH OCTANTS CE	2075	545	2.1600	136	46.29	1.306	2.0638×10^6
One OCT CE One OCT ENC	2075	545	2.1600	136	46.29	1.278	2.0127×10^6

Table 5.3 Flow reduction comparison

CASE	PRESSURE PSIA	TEMPERATURE °F	FLOW 10^6 lbm/ hr-ft ³	POWER % of Full Power	DENSITY lbm/ft ³	MDNBR 1.3 W-3 CHF Correlation	FLOW OUT OF "Hot" Channel lbm/hr-ft ³
BOTH OCTANTS CE	2075	545	2.0520	131.8	46.29	1.299	1.9654×10^6
One Oct CE One Oct ENC	2075	545	2.0520	131.8	46.29	1.270	1.9654×10^6

Table 5.4 Density reduction comparison

CASE	PRESSURE PSIA	TEMPERATURE °F	FLOW 10 ⁶ lbm/ hr-ft ³	POWER % of Full Power	DENSITY lbm/ft ³	MDNBR 1.3 W-3 CHF Correlation	FLOW OUT OF "Hot" Channel lbm/hr-ft ³
BOTH OCTANTS CE	2400	580	2.1600	122.2	43.88	1.307	2.0914x10 ⁶
One Oct CE One Oct ENC	2400	580	2.1600	122.2	43.88	1.272	2.0408x10 ⁶

10^6 lbm/hr-ft². The inlet density was 43.88 lbm/ft³. For these conditions with mixed grids, the minimum DNBR was 1.272 and the "hot" channel exit flow was reduced by 2.4% to 2.0408×10^6 lbm/hr-ft².

E. Conclusion

Based on the dual octant modeling, using two different grid spacer types on adjacent assemblies does impact the amount of cross-flow. This means that a "hot" channel could experience a flow reduction under certain conditions. Since this is only a concern for the "hot" assembly in the core, a careful loading pattern could eliminate the problem. This reduction could also be accounted for by the proper thermal hydraulic model.

A multistage code such as D-TORC could model the crossflow behavior if the option for assembly by assembly variation of grid loss coefficients was incorporated. If this is not available, then a flow penalty could be applied to the "hot" assembly.

The flow reduction case, the density variation case and the overpower case, showed flow reductions of 2.3, 2.4, and 2.5%, respectively. These bounded the zero power case which exhibited a flow reduction of 1%. From these cases, an inlet flow penalty of 2.5% could be applied to the hot assembly.

VI. CONCLUSIONS AND SUGGESTIONS FOR FUTURE WORK

A. Conclusions

The following are conclusions and observations from this study:

1. A small thermal-hydraulics model was developed and verified as valid for a specific use.
2. If a small model is going to be used extensively, cost benefits can be achieved by optimizing the routine for minimum computation time.
3. A minimal T-H model could have considerable value without describing the core in any detail.
4. Extensive planning and preparation are necessary for very large thermal-hydraulics models. These models are expensive to run. Costs related to optimizing may be more than the actual runs.
5. The large model grid spacer study showed that assembly to assembly flow starvation was related to the variance in grid loss coefficients.
6. Results from this study show that thermal hydraulics models should take into account differences in grid loss coefficients.

B. Suggestions for Future Work

As specific problems arise, the development of T-H models to address them can be of considerable benefit to users.

The very small T-H model used for verification work, could be further verified and confirmed for actual setpoint generation.

The study of the effect of the grids on cross flow was only conducted for one variable at a time. Further work needs to address questions such as: what is the effect of combinations of the parameters? Also, both assemblies were considered to have the same power. In actual loading patterns, the powers of adjacent assemblies can be different. This parameter coupled with some of the other considerations, may induce additional flow "starvation" in a "hot" assembly and reduce the margin to DNB. Therefore, power differences and their effects could be another area for future analysis.

VII. LITERATURE CITED

1. Tong, L. S., and Joel Weisman. 1979. Thermal Analysis of Pressurized Water Reactors. American Nuclear Society, LaGrange Park, Illinois.
2. Rowe, D. S. 1973. COBRA-III-C: A Digital Computer Program for Steady State and Transient Thermal-Hydraulic Analysis of Rod Bundle Nuclear Fuel Elements. Battelle-Northwest, Richland, Washington.
3. Stewart, C. W., C. L. Wheeler, R. J. Cena, C. A. McMonagle, J. M. Cuta, D. S. Trent. 1977. COBRA-IV-1: The Model and the Method. Battelle Pacific Northwest Laboratories, Richland, Washington.
4. Wheeler, C. L., C. W. Stewart, R. J. Cena, D. S. Rowe, A. M. Sutey. 1976. COBRA-IV-1: An Interim Version of COBRA for Thermal Hydraulic Analysis of Rod Bundle Nuclear Fuel Elements and Cores. Battelle Pacific Northwest Laboratories, Richland, Washington.
5. Moreno, P., C. Chiu, R. Bowring, E. Khan, J. Liu, N. Todreas. 1977. Methods for Steady State Thermal/Hydraulic Analysis of Pressurized Water Reactor Cores. Energy Laboratory Report No. MIT-EL 76-006. Massachusetts Institute of Technology.
6. Stewart, C. W., J. N. Cuta, A. S. Koontz, J. M. Kelly, K. L. Basehore, T. L. George, D. S. Rowe. 1981. VIPRE Code Manual, Volumes 1-5. Electric Power Research Institute. Palo Alto, California.
7. Stewart, C. W. 1975. XCOBRA-III-C: A Computer Code to Determine the Distribution of Coolant During Steady State and Transient Core Operation. Exxon Nuclear Company, Inc., Richland, Washington.
8. Stewart, C. W. 1975. TORC Code: A Computer Code for Determining the Thermal Margin of a Reactor Core. Combustion Engineering, Windsor, Connecticut.
9. CETOP: Thermal Margin Model Development. 1981. Combustion Engineering, Windsor, Connecticut. CENTSD-150-P, May, 1981.

10. Tong, L. S. 1969. "Critical Heat Fluxes in Rod Bundles," Two Phase Flow and Heat Transfer in Rod Bundles, V. E. Schrock, Ed., American Society of Mechanical Engineers, New York.
11. Gellerstedt, T. J. S., R. A. Lee, W. J. Overjohn, R. H. Wilson, L. I. Stanek. November, 1966. "Correlation of Critical Heat Flux in a Bundle Cooled by Pressurized Water." Two Phase Flow and Heat Transfer in Rod Bundles, Symposium Proceedings of Winter Annual Meeting of the American Society of Mechanical Engineers, Los Angeles, California, pp. 63-71.
12. "CE Critical Heat Flux." 1976. Part 1, CENPD-162 B-A; Part 2, CENPD-207-P. Combustion Engineering, Windsor, Connecticut.
13. Gupta, R. N. 1976. Maine Yankee Core Thermal-Hydraulic Model Using COBRA-III-C. Yankee Atomic Company, Westborough, Massachusetts.
14. Chunis, J. A. 1977. COBRA-III-C user Manual for NUSCO Thermal Hydraulic Analysis of Pressurized Water Reactors. Northeast Utilities, Hartford, Connecticut.
15. Chunis, J. A. 1976. CE-Setpoint Methodology. Combustion Engineering, Windsor, Connecticut.
16. Apley, W. 1980. Review of ENC Cycle 6 TM/LP Analysis for Fort Calhoun. Battelle Northwest Laboratories, Richland, Washington.
17. Fort Calhoun Station Unit No.1, Updated Safety Analysis Report. NRC Docket No. 50-285, Omaha Public Power District.
18. TORC-Code: Verification and Simplified Modeling Methods. January, 1977. CENPD-206-P, Combustion Engineering, Windsor, Connecticut.
19. Fort Calhoun Station Unit No. 1, Operating License DPR-40 and and Technical Specifications, Omaha Public Power District.
20. Tong, L. S. 1967. "Prediction of Departure from Nucleate Boiling for an Axially Non-uniform Heat Flux Distribution," J. Nuclear Energy, 21, pp. 241-248.

21. Tong, L. S. 1972. "Boiling Crisis and Critical Heat Flux,"
Critical Review Series, pp. 30, 42, U. S. Atomic Energy
Commission, Washington, D.C.
22. "Single Phase Hydraulic Performance of Exxon Nuclear and
Combustion Engineering Fort Calhoun Fuel Assemblies."
March, 1979. XN-NF-79-1b.

VIII. ACKNOWLEDGMENTS

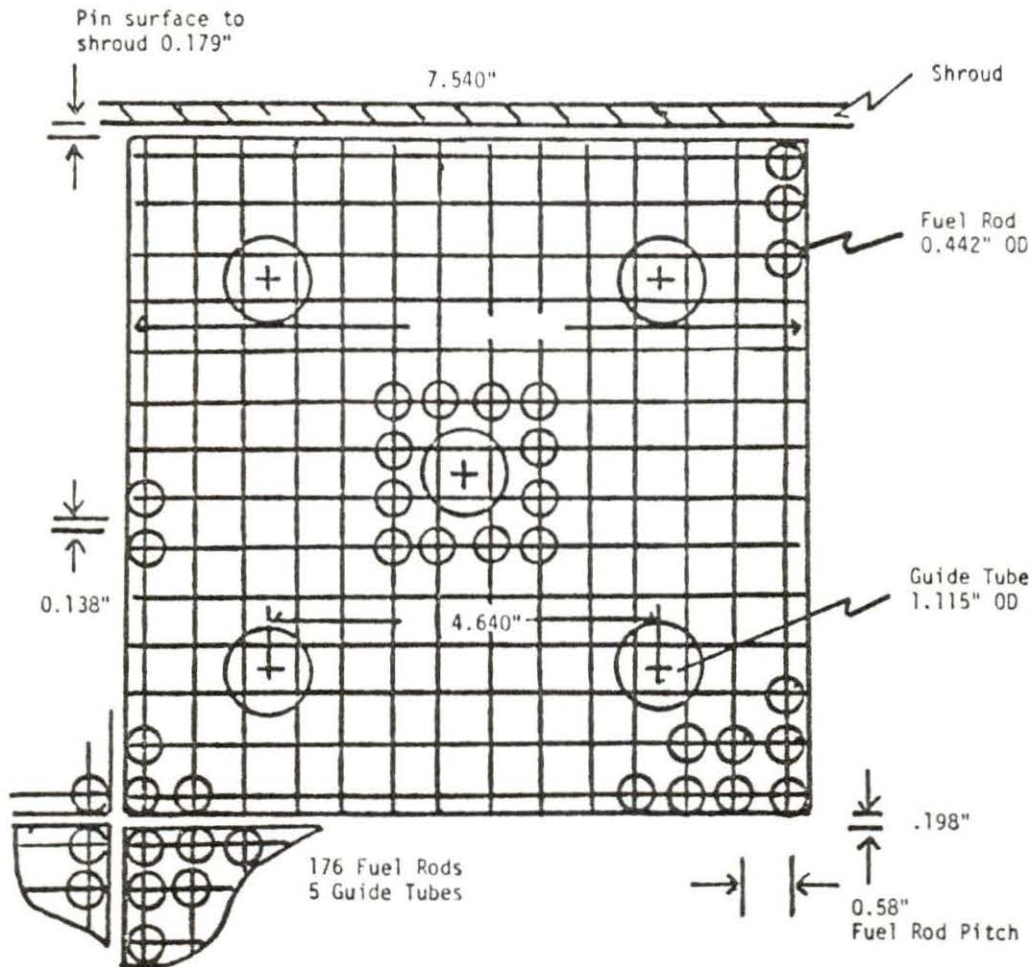
I would like to express my appreciation to my major professor, Dr. Richard Danofsky, for his support and guidance that was provided through completion of the thesis. The Omaha Public Power District, in particular Dr. Joseph K. Gasper, provided technical expertise and financial support. Without this assistance, the project would not have seen completion. In addition, the research assistantship provided by Power Affiliates was highly valued.

IX. APPENDIX A: EXXON NUCLEAR COMPANY FUEL DATA

Table 9.1 Key neutronic design parameters for Fort^a Calhoun XN-1 type H fuel

<u>Standard Fuel Assembly</u>	
Enrichment, w/o U-235	3.50
Number of Fuel Pins, H ₂ O	176
Fuel Pin Array	14 x 14
Fuel Assembly Pitch, in.	8.18
Fuel Rod Pitch, in.	.580
Active Fuel Length, in.	128.0
Fuel Pellet OD, in.	0.370
Clad OD, in.	0.442
Clad ID, in.	0.378
Guide Tube OD, in.	1.115
Guide Tube ID, in.	1.035
Theoretical Fuel Density, % of 10.96 gm/cc	94.0

^aSN-NF-69 Fort Calhoun Reload Fuel Design Report Mechanical, Thermal Hydraulic and Neutronic Analyses, September, 1979. Exxon Nuclear Company, Inc., Richland, Washington.



Blockage Area

$$\text{Fuel Rod Blockage} = 176 \times \pi \times \left(\frac{0.442}{2}\right)^2 = 27.01 \text{ in}^2$$

$$\text{Guid Tube Blockage} = 5 \times \pi \times \left(\frac{1.115}{2}\right)^2 = 4.8821 \text{ in}^2$$

Figure 9.1 ENC fuel assembly geometry

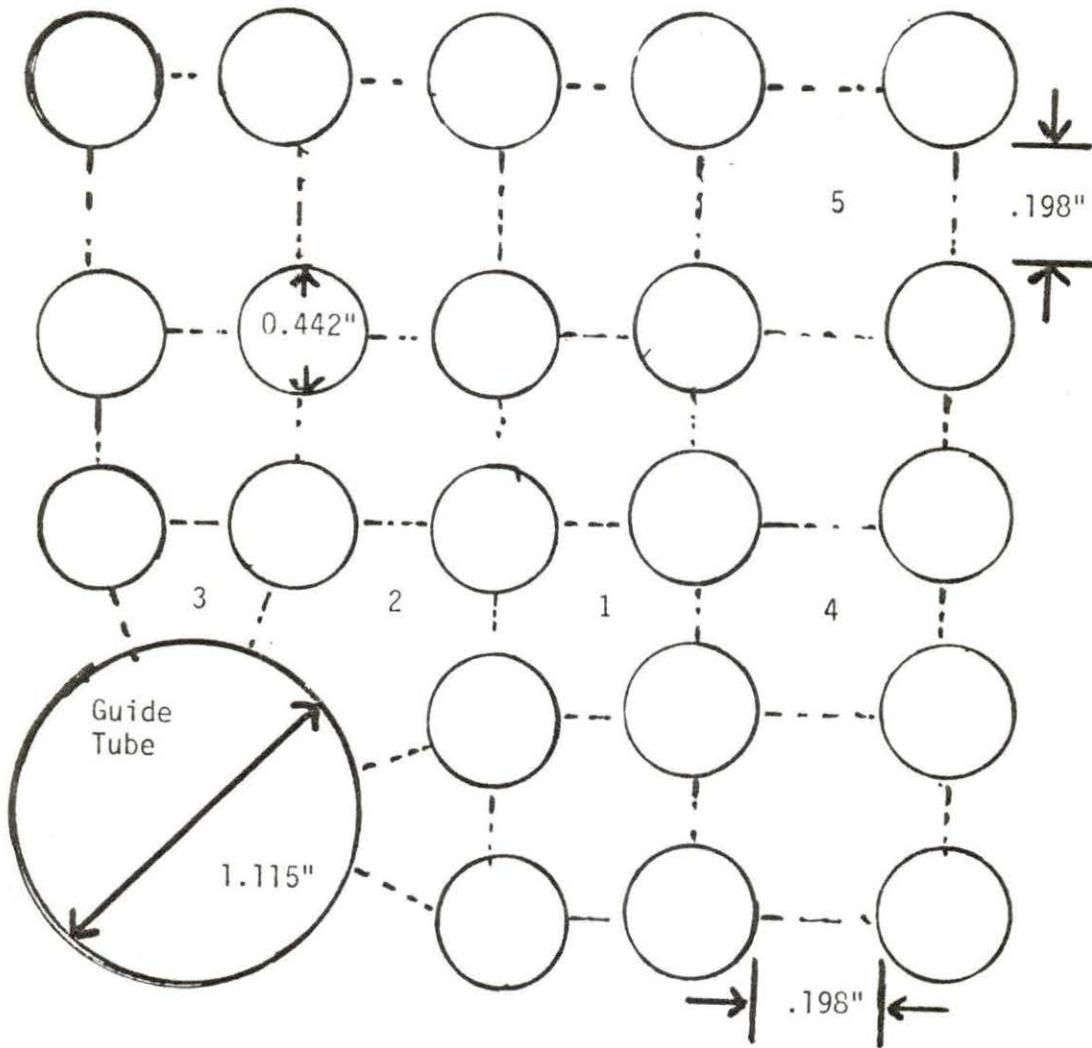


Figure 9.2 ENC hot assembly flow areas

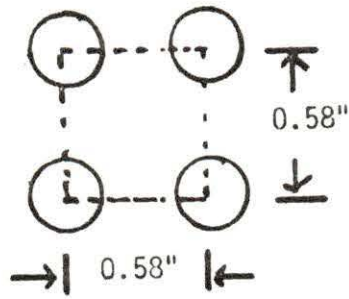


Figure 9.3 ENC matrix subchannel

Flow Area (A_F)

$$A_F = (0.58)^2 - \left(\frac{\pi}{4}\right) (.442)^2 = 0.1830 \text{ inches squared}$$

Heated Perimeter (HP)

$$HP = (.442) \pi = 1.389 \text{ inches}$$

Wetted Perimeter (WP)

$$WP = HP = 1.389 \text{ inches}$$

Hydraulic Diameter (D_H)

$$D_H = \frac{4 (A_F)}{WP} = \frac{4 (.1830)}{1.389}$$

$$D_H = .5272 \text{ inches}$$

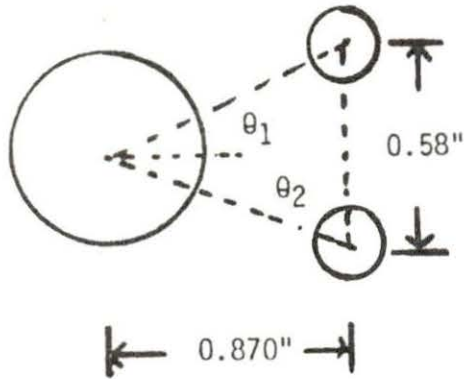


Figure 9.4 ENC side subchannel

The rod OD = .442". The guide tube diameter = 1.115"

$$\theta_1 = \tan^{-1} \frac{0.290}{0.870} = 18.43^\circ \quad \theta_2 = 90 - \theta_1 = 71.5^\circ$$

Flow Area (A_F)

$$A_F = 1/2(.58)(.87) - 2 \left(\frac{\pi}{4} \right) (.442)^2 \left(\frac{71.57}{360} \right) - \left(\frac{\pi}{4} \right) (1.115)^2 2 \left(\frac{18.43}{360} \right)$$

$$A_F = 0.0913 \text{ inches square}$$

Heated Perimeter (HP)

$$HP = .442 (\pi) \left(\frac{71.57}{360} \right) (2) = 0.5521 \text{ inches}$$

Wetted Perimeter (WP)

$$WP = (1.115) \pi (2) \left(\frac{18.43}{360} \right) + HP$$

$$WP = 0.9108 \text{ inches}$$

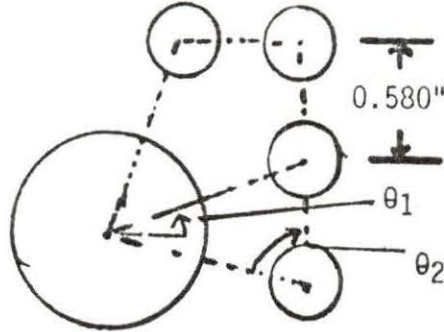


Figure 9.5 ENC corner subchannel

The rod diameter equals .442 inches.

The guide tube diameter equals 1.115 inches,

$$\theta_1 = 18.43^\circ \quad \theta_2 = 71.57^\circ$$

Flow Area (A_F)

$$A_F = (0.870)^2 - 1.25 \left(\frac{\pi}{4}\right) (0.442)^2 - \frac{\pi}{4} (1.115)^2 (.25) - .0913 \text{ inches}$$

$$A_F = 0.2297 \text{ inches}$$

Heated Perimeter (HP)

$$HP = (0.442) \frac{\pi(3(90) + 2(18.43))}{360}$$

$$HP = 1.184 \text{ inches}$$

Wetted Perimeter (WP)

$$WP = (1.115) \frac{\pi(\theta_2 - \theta_1)}{360} + HP = (1.115) \pi \frac{(71.57 - 18.36)}{360} + 1.184$$

$$WP = 1.701 \text{ inches}$$

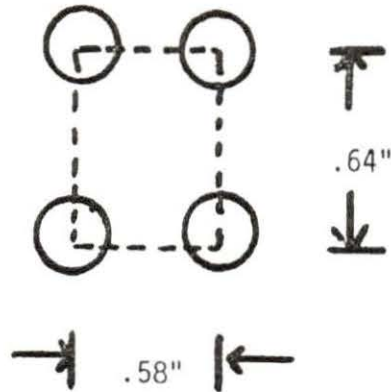


Figure 9.6 Subchannel between two ENC assemblies

The diameter of all rods is .442 inches.

Flow Area (A_F)

$$A_F = (.64) (.58) - \left(\frac{\pi}{4}\right) (.442)^2$$

$$A_F = 0.2178 \text{ inches squared}$$

Heated Perimeter (HP)

$$HP = \pi(.442) = 1.389 \text{ inches}$$

Wetted Perimeter (WP)

$$WP = HP = 1.389 \text{ inches}$$

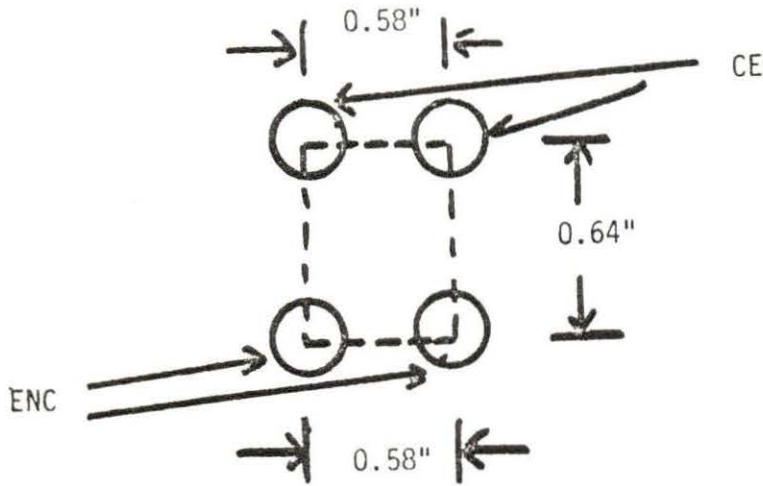


Figure 9.7 Subchannel between one ENC assembly and one CE assembly

The rod diameter of a CE rod is .440 inches.

The rod diameter of an ENC rod is .442 inches.

Flow Area (A_F)

$$A_F = (.64) (.58) - \left(\frac{\pi}{4}\right) (.442)^2 (.5) - \frac{\pi}{4} (.440)^2 (.5)$$

$$A_F = 0.2185 \text{ inches squared}$$

Heated Perimeter (HP)

$$HP = \pi (.442) (.5) + \pi (.440) .5$$

$$HP = 1.385 \text{ inches}$$

Wetted Perimeter (WP)

$$WP = HP = 1.385 \text{ inches}$$

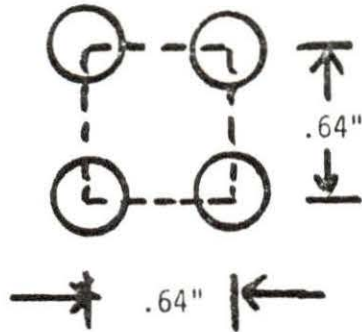


Figure 9.8 Subchannel surrounded by four ENC assemblies

The diameter of all rods is .442 inches.

Flow Area (A_F)

$$A_F = (.64)^2 - \frac{\pi}{4} (.442)^2$$

$$A_F = 0.2562 \text{ inches squared}$$

Heated Perimeter (HP)

$$HP = \pi (.442)$$

$$HP = 1.389 \text{ inches}$$

Wetted Perimeter (WP)

$$WP = HP = 1.389 \text{ inches}$$

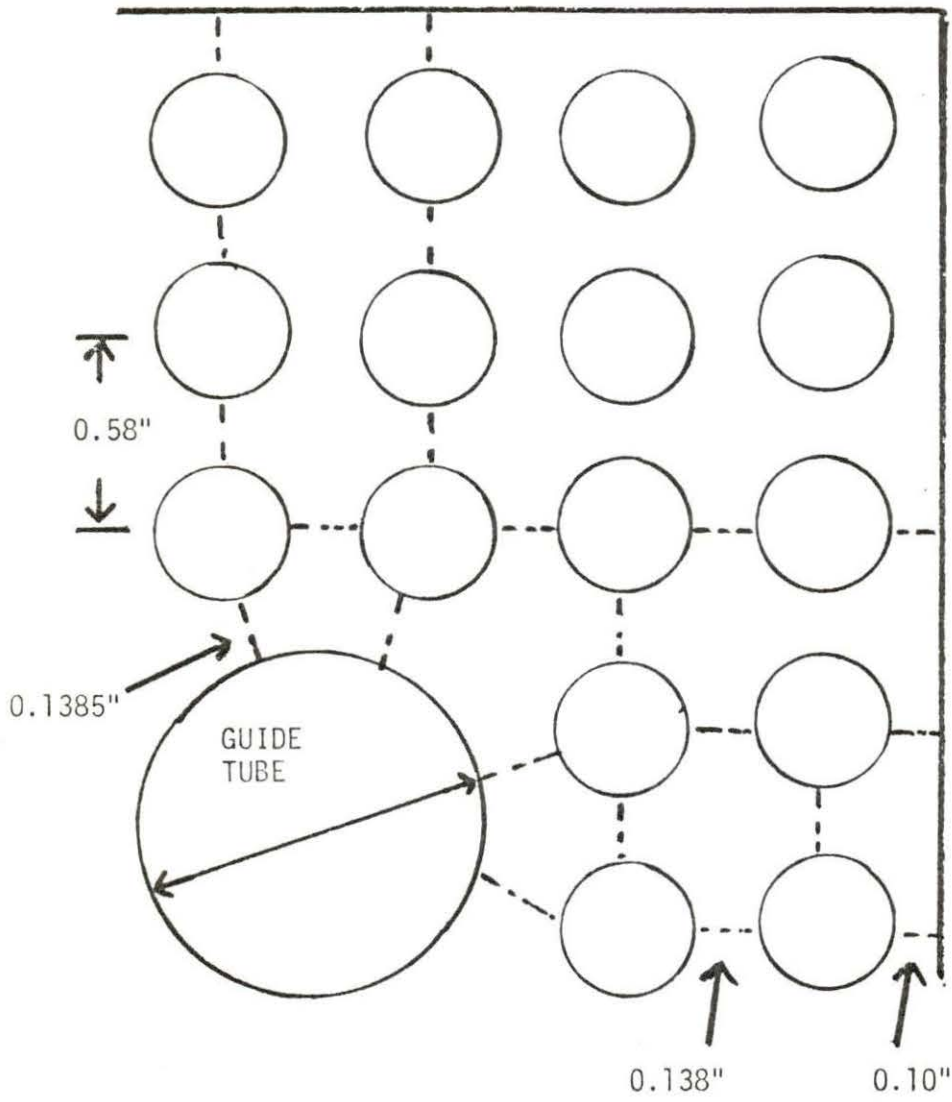


Figure 9.9 ENC gap connections

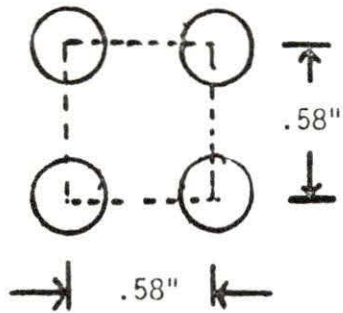


Figure 9.10 ENC matrix subchannel gap connections

The rod diameter for ENC fuel is .442 inches.

GAP Spacing (GS)

$$GS = .58 - .442 = .138$$

$$GS = 0.138 \text{ inches}$$

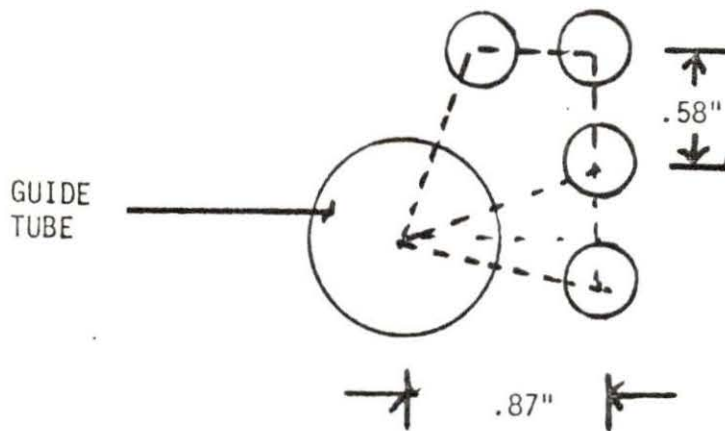


Figure 9.11 ENC gap connections for side and corner subchannels

The rod diameter for ENC fuel is .442 inches.

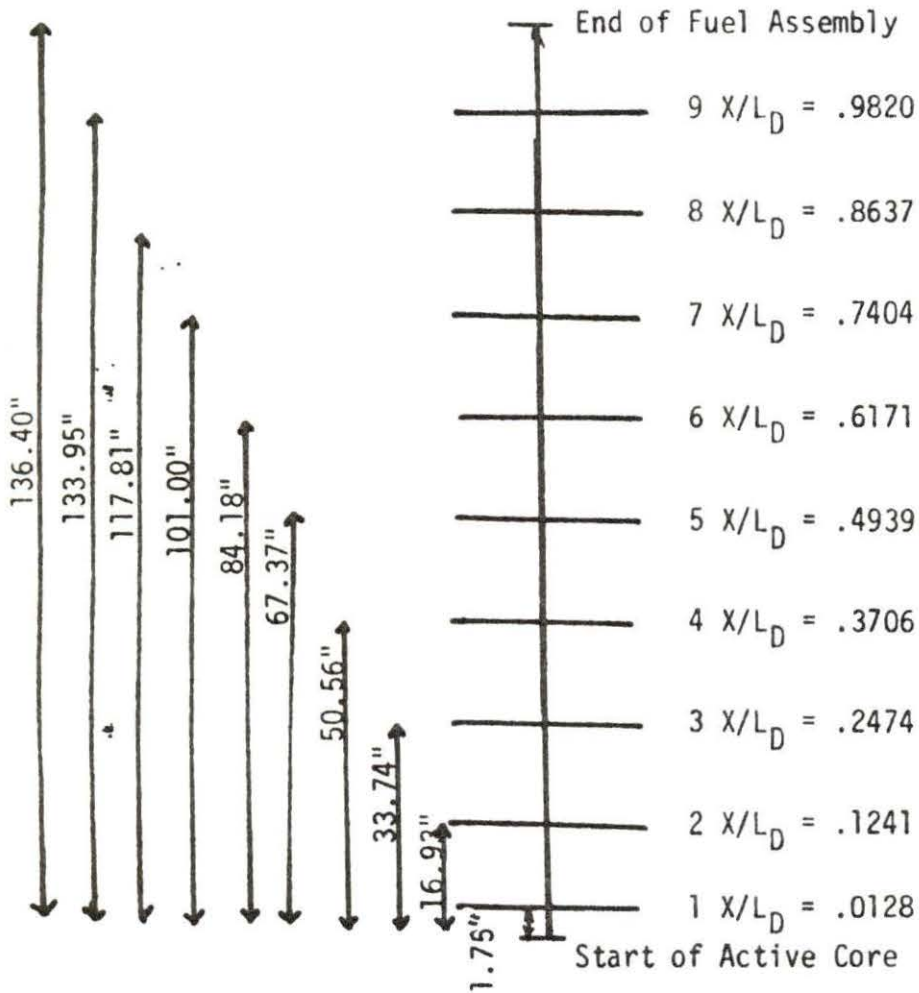
The guide tube diameter is 1.115 inches.

GAP Spacing (GS)

$$GS = (.87^2 + (\frac{.58}{2})^2)^{1/2} - \frac{.442}{2} - \frac{1.115}{2}$$

$$GS = 0.1385 \text{ inches}$$

Nominal Spacer Grid Thickness = 2,000"
 Note: Dimensions Refer to the Base of Spacer Grid



EXXON DESIGN DRAWINGS

XN-302, 568

XN-NF-303, 253

Figure 9.12 Relative spacer grid locations

X. APPENDIX B: COMBUSTION ENGINEERING FUEL DATA

Table 10.1 Key neutronic design parameters for Fort Calhoun CE type G fuel

Enrichment, w/o U-235	3.03
Number of Fuel Pins	176
Fuel Pin Array	14 x 14
Fuel Assembly Pitch in.	8.18
Fuel Rod Pitch in.	.58
Active Fuel Length in.	128
Fuel Pellet OD in.	.3815
Clad OD in.	.44
Clad ID in.	.388
Guide Tube DD in.	1.115
Guide Tube ID in.	1.035
Theoretical Fuel Density %	93.5 \pm 1.5

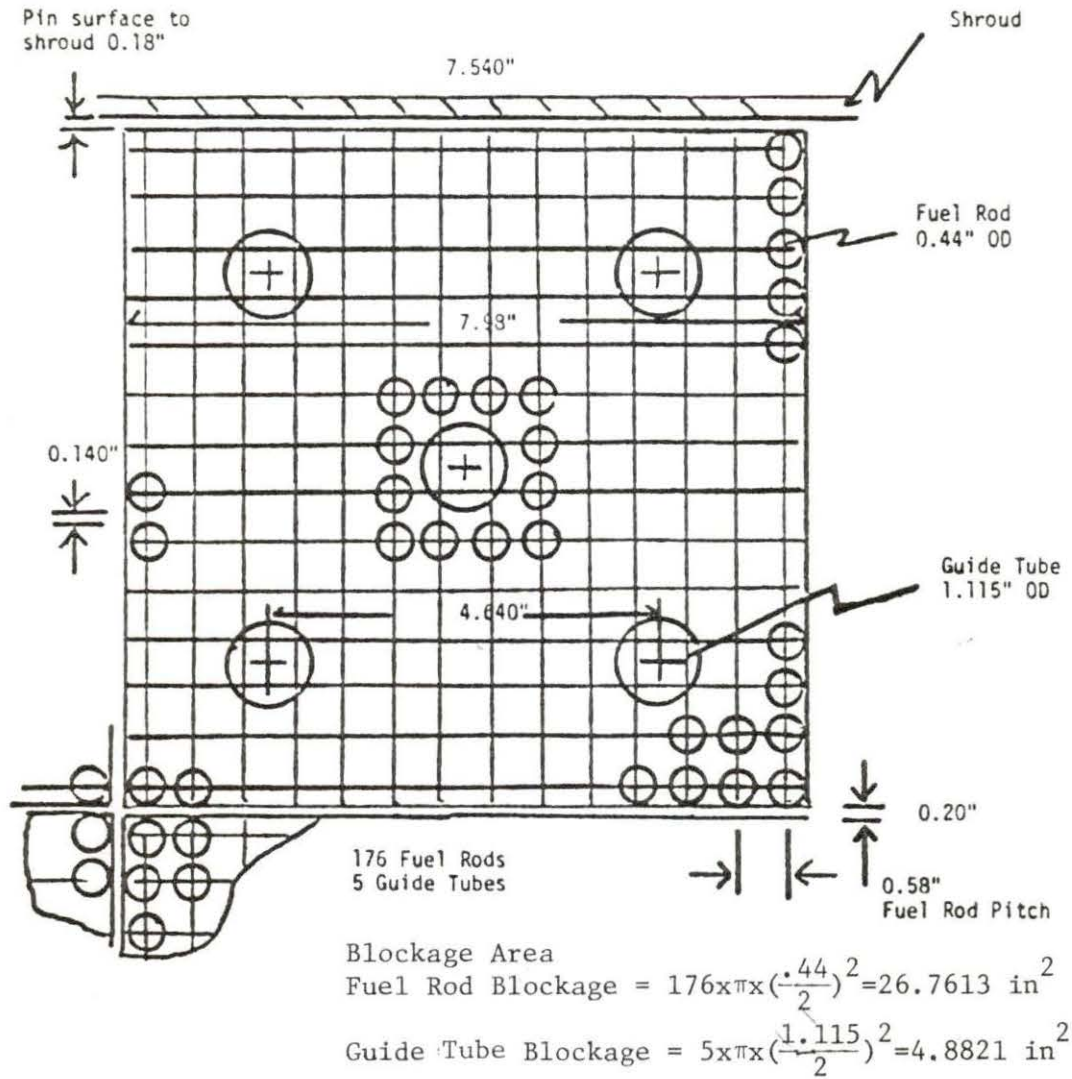


Figure 10.1 CE fuel assembly geometry

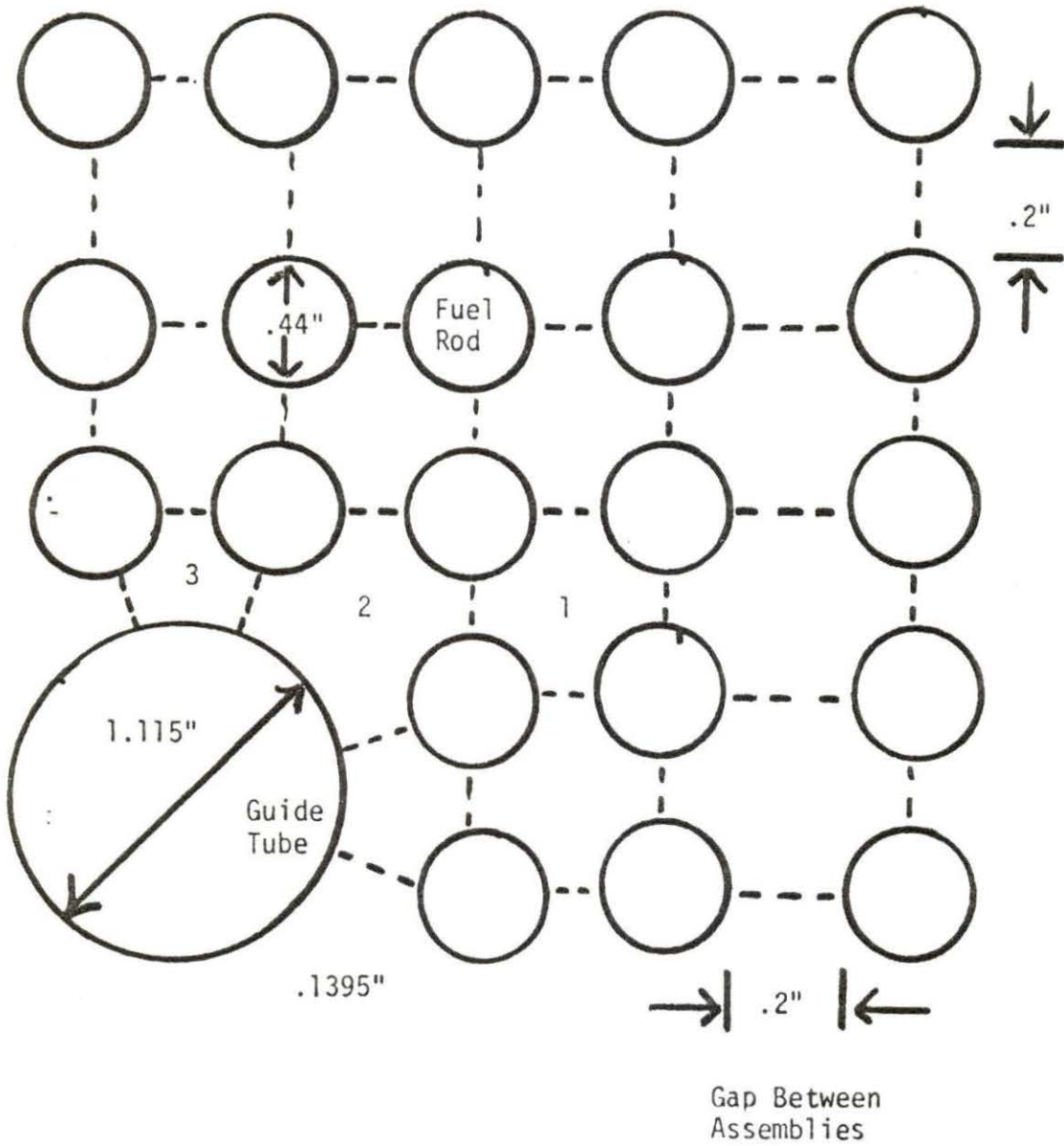


Figure 10.2 CE hot assembly flow areas

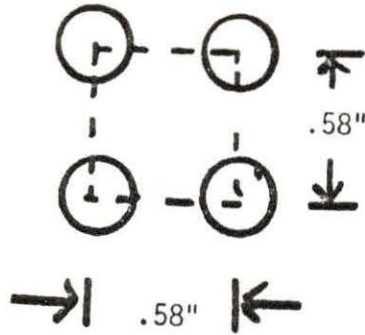


Figure 10.3 CE matrix subchannel

Flow Area (A_F)

$$A_F = (.58)^2 - \left(\frac{\pi}{4}\right)(.44)^2 = 0.1843 \text{ inches square}$$

Heated Perimeter (HP)

$$HP = (.44)\pi = 1.382 \text{ inches}$$

Wetted Perimeter (WP)

$$WP = HP = 1.382 \text{ inches}$$

Hydraulic Diameter (D_H)

$$D_H = \frac{4(A_F)}{WP} = \frac{4(.1843)}{1.382}$$

$$D_H = .5334 \text{ inches}$$

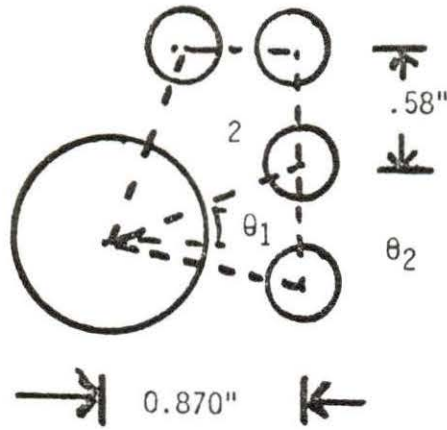


Figure 10.4 CE side subchannel

The diameter of the fuel rod is equal to .44 inches.

The diameter of the guide tube is equal to 1.115 inches.

$$\theta_1 = 18.43^\circ \quad \theta_2 = 71.57^\circ$$

Flow Area (A_F)

$$A_F = (.87) (.29) - \frac{2\theta_1}{360} \left(\frac{\pi}{4}\right) (1.115)^2 - \frac{2\theta_2}{360} \left(\frac{\pi}{4}\right) (.44)^2$$

$$A_F = 0.918 \text{ inches squared}$$

Heated Perimeter (HP)

$$HP = \frac{2\theta_2}{360} \pi (.44)$$

$$HP = .5496 \text{ inches}$$

Wetted Perimeter (WP)

$$WP = HP + \frac{2\theta_1}{360} (\pi) (1.115)$$

$$WP = .9083 \text{ inches}$$

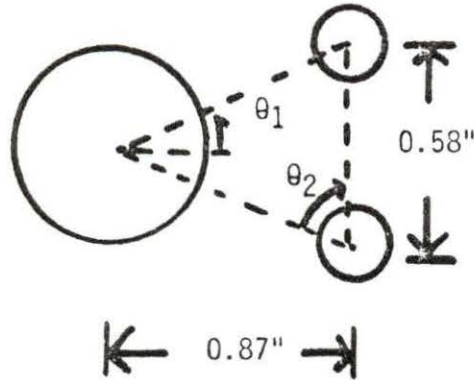


Figure 10.5 CE corner subchannel

The rod diameter is equal to .44 inches.

The guid tube diameter is equal to 1.115 inches

$$\theta_1 = 18.43^\circ \quad \theta_2 = 71.57^\circ$$

Flow Area (A_F)

$$A_F = (0.87)^2 - 1.25 \left(\frac{\pi}{4} \right) (0.44)^2 - \frac{\pi}{4} (1.115)^2 - 0.0918$$

$$A_F = .2309 \text{ inches squared}$$

Heated Perimeter (HP)

$$HP = (.44) \frac{\pi(3(90) + 2(18.43))}{360}$$

$$HP = 1.178 \text{ inches}$$

Wetted Perimeter (WP)

$$WP = HP + \frac{(\theta_2 - \theta_1)}{360} (1.115)\pi$$

$$WP = 1.695 \text{ inches}$$

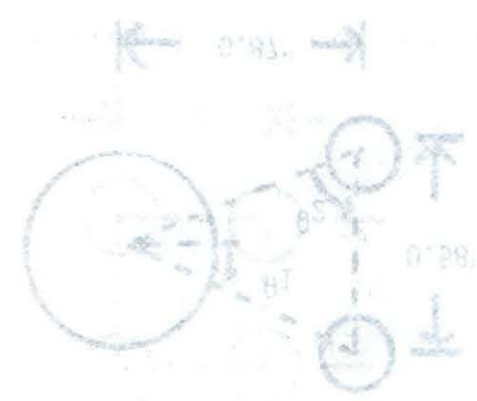
$$M = 10 + \frac{300}{(1.5 + 0.5)} \quad (1)$$

$$M = 10 + \frac{300}{2} = 155 \quad (2)$$

$$M = 10 + \frac{300}{2} = 155 \quad (3)$$

$$M = 10 + \frac{300}{2} = 155 \quad (4)$$

The above diagram shows the forces acting on the beam. The reaction at the support is 155. The weight of the beam is 10. The distance between the support and the weight is 1.5. The distance between the support and the reaction is 2.0.



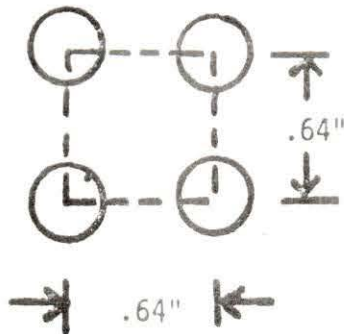


Figure 10.6 Subchannel surrounded by four CE assemblies

The rod diameter of the CE fuel is .440 inches.

Flow Area (A_F)

$$A_F = (.64)^2 - \frac{\pi (.44)^2}{4}$$

$$A_F = 0.2575 \text{ inches squared}$$

Heated Perimeter (HP)

$$HP = \pi (.440)$$

$$HP = 1.382 \text{ inches}$$

Wetted Perimeter (WP)

$$WP = HP = 1.382 \text{ inches}$$